



# Direct conversion of the water adsorption energy to electricity on the surface of zirconia nanoparticles

A. S. Doroshkevich<sup>1,2</sup> · E. B. Asgerov<sup>1,3</sup> · A. V. Shylo<sup>2</sup> · A. I. Lyubchik<sup>4</sup> · A. I. Logunov<sup>5</sup> · V. A. Glazunova<sup>6</sup> · A. Kh. Islamov<sup>1</sup> · V. A. Turchenko<sup>1,2</sup> · V. Almasan<sup>7</sup> · D. Lazar<sup>7</sup> · M. Balasoiu<sup>1,8</sup> · V. S. Doroshkevich<sup>9</sup> · A. I. Madadzada<sup>1,3</sup> · Kh. T. Kholmurodov<sup>1,5</sup> · V. I. Bodnarchuk<sup>1</sup> · B. L. Oksengendler<sup>10</sup>

Received: 21 November 2018 / Accepted: 11 February 2019  
© King Abdulaziz City for Science and Technology 2019

## Abstract

Based on the example of a nanopowder system  $ZrO_2$ -3% mol  $Y_2O_3$  with atmospheric humidity interaction, the possibility of exothermic heterophase electrochemical energy conversion to electric energy is shown. Electrical properties and structure of the experimental sample were studied under gradient molecular flux density of humidity during sample saturation. The idea of development of the novel chemo-electronic converter device based on nanoscale dielectrics as  $ZrO_2$ -3% mol  $Y_2O_3$  is proposed.

**Keywords** Powder nanotechnology · Humidity to electricity · Chemo-electronic conversion · Adsorption phase transition · Electronic processes · Physical chemistry of surface

## Introduction

Specific physical and chemical properties of the surface of nanosized oxide particles are of interest of a number of modern scientific trends. Novel scientific and technical

applications of phenomena and processes occurred on such surface are connected with nanotechnology. The science of surface is associated with the study of structural properties of surfaces and adsorbates, and corresponding mechanisms of reactions on a surface (Konstantinova et al. 2011;

✉ A. S. Doroshkevich  
doroh@jinr.ru

E. B. Asgerov  
elmar.asgerov@gmail.com

A. V. Shylo  
art.shylo@gmail.com

A. I. Lyubchik  
andrey.lyubchik@campus.fct.unl.pt

A. I. Logunov  
fizikaman26@gmail.com

V. A. Glazunova  
matscidep@aim.com

V. Almasan  
almasanvaler@yahoo.com

M. Balasoiu  
masha.balasoiu@gmail.com

V. S. Doroshkevich  
v.doroshkevich@donnu.edu.ua

B. L. Oksengendler  
oksengendlerbl@yandex.ru

<sup>1</sup> Joint Institute for Nuclear Research, Dubna, Russia

<sup>2</sup> Donetsk Institute for Physics and Engineering named after O.O. Galkin, Kiev, Ukraine

<sup>3</sup> National Center for Nuclear Research, Baku, Azerbaijan

<sup>4</sup> i3N/CENIMAT, Department of Materials Science, Faculty of Science and Technology, New University of Lisbon and CEMOP/UNINOVA, Caparica, Portugal

<sup>5</sup> Dubna State University, Dubna, Russia

<sup>6</sup> Donetsk Institute for Physics and Engineering named after O.O. Galkin, Donetsk, Ukraine

<sup>7</sup> National Institute for Research and Development of Isotopic and Molecular Technologies Cluj, Napoca, Romania

<sup>8</sup> Horia Hulubei National Institute for R&D in Physics and Nuclear Engineering, Bucharest, Romania

<sup>9</sup> Donetsk National University, Donetsk, Ukraine

<sup>10</sup> Institute of Ion-Plasma and Laser Technologies named after U.A. Arifov Academy of Sciences of the Republic of Uzbekistan, Tashkent, Uzbekistan

Zainullina and Zhukov 2001). All steps of interaction of an atomic particle with a surface as adhesion, surface reactions and desorption include the energy transfer between adsorbate and the surface of solid matter (Kammler and Kuppers 1999). In case of atomic particles, which are actively interacting with surface atoms (chemical sorption) or with each other (recombination of radicals, heterogeneous catalytic reactions), the energy transferred to the solid is the energy that released by acts of reactionary collisions at the surface. During reactionary collisions, energy exchange usually proceeds through the stage of formation of vibrationally and electronically excited intermediate quasimolecular particles on a surface. The excited states of adsorbates related to rotational, vibrational and electronic degrees of freedom are involved in most of dynamic processes. Their nature and relaxation types are the subject of a new scientific direction of research at the interface of surface physics, physics of atomic collisions and chemical physics named “Chemovoltatics” (Kabansky et al. 1979, 2004; Styrov et al. 2011; Styrov and Simchenko 2012). Thus, chemovoltatics studies the energy exchange between a solid matter and slow atomic particles that strike the surface. By slow atomic particles, we usually mean simple molecules, radicals, ions or atoms whose kinetic energy is comparable to the energy of phonons of a solid matter and much less than the energy of other elementary excitations in a solid (Styrov and Tyurin 2003). The perspectives of chemo-electricity production become possible with the development of nanotechnology. Tyurin et al. (2008) and Styrov and Tyurin (2003) have obtained the chemo-electromotive force (EMF) about 2 mV and current up to 700 nA during the interaction of hydrogen atoms with the nanostructured surface of SiC crystals. For a solar cell of a tandem type, this power can be considered as a contribution to the efficiency increase.

The mechanisms of chemo-electronic emission and ways to improve the efficiency of chemo-electronic converters are being actively studied. The criteria on which functional nanomaterials should be selected are established. According to Tyurin et al. (2008), a small depth of adsorption level positions  $E_a \leq 0.2\text{--}0.4$  eV is sufficient for generation of high yield of electrons. Small levels provide preferential adsorption of atoms in a charged form and allow to avoid the neutralization reaction. It was shown (Gergen et al. 2001; Styrov and Simchenko 2013) that to reduce the fraction of heat losses, it is necessary to reconcile between the heat of chemical reaction of molecules with the surface of a solid and its width of the band gap  $E_g$ . Based on relatively high dissociation and ionization energies of molecules in a gas phase, it follows that materials with a large band gap will be the most efficient for chemo-electronic conversion. For example, taking into account the dissociation energy  $D_g =$

4.48 eV of the model gas—H<sub>2</sub> hydrogen the value of the bandgap width of sorbent materials can be estimated.

During the past years, attention to the engineering of the electronic structure of surface layers of adsorbates, as a method to control processes involved electrons, is increased. Several models of the Tamm state modification for the nanoscale level have been proposed and new properties of electronic structure of nanoparticles have been demonstrated. Particularly, the following can be identified: elongation of Tamm’s orbitals outside the particle with a decrease of its size (Oksengendler et al. 2014) (formation of chemically uncompensated valence orbitals called “dangling bonds” capable of “capturing” incoming molecules from a gas phase); an increase of the Coulson free valence index of Tamm orbitals with increase of the surface curvature (Oksengendler et al. 2010a, b); displacement of a pair of Tamm state levels to the middle of the bandgap with the increases of the nanoparticles surface curvature in ionic crystals (decrease of effective width of the bandgap) (Oksengendler et al. 2016); decrease of the electron localization energy with the warp of energy bands as a result of the surface charging by adsorbates (collapse of the band gap during adsorption of water molecules) (Okamoto 2008; Subhoni et al. 2018). As a result, work devoted to the photoelectric properties of solar cells based on perovskites shows an increase of the photocurrent (to 1.3%) only by replacing the planar interfaces of the functional structures to nanoscale structures with the total identity of all the other elements (Zheng et al. 2014). Preliminary analysis of these results showed that the cause of such effect is apparently related to the features of Tamm states on the fractal interface. It should be noted that a similar effect has been previously observed for silicon (Muller et al. 2004). Thus, there is a reason to believe that further optimization of functional materials for chemo-electronic converters in terms of energy characteristics and the form of phase boundaries will increase the efficiency of conversion of chemical energy into an electrical form.

At the nanoscale, the system ZrO<sub>2</sub>–Y<sub>2</sub>O<sub>3</sub> has a high density of low-energy localized electronic states with an energy of 0.1–0.8 eV in the near-surface region and the electron work function over 3–5 eV (Ptitsyn 2007; Zainullina and Zhukov 2000); therefore, this is a promising functional material for chemo-electronic conversion.

## Materials and methods

For the production of ZrO<sub>2</sub>–Y<sub>2</sub>O<sub>3</sub> nanopowders (Fig. 1), a chemical technology of co-precipitation was used (Konstantinova et al. 2011; Doroshkevich et al. 2006). First, hydrated zirconium hydroxide was precipitated from a chloride raw

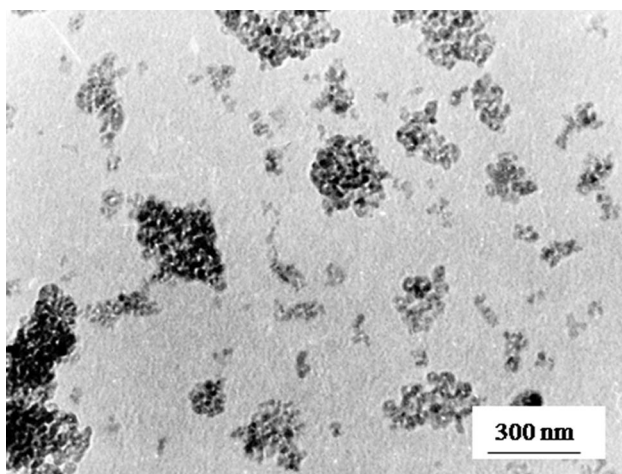


**Fig. 1** TEM image of  $\text{ZrO}_2$ -3 mol%  $\text{Y}_2\text{O}_3$ , 400 °C, 2 h nanopowder

material. Then, the obtained material undergoes dehydration in a specialized microwave oven ( $T=120\text{ °C}$ ,  $t=0.4\text{ h}$ ). After which, the amorphous powder was subjected to crystallization annealing at a temperature of 400 °C for 2 h.

To obtain an experimental device of chemo-electronic converter, a suspension of a 1% water solution of polyvinyl alcohol (PVA) polymer with a nanopowder  $\text{ZrO}_2$ -3% mol  $\text{Y}_2\text{O}_3$  (particle size 7.5 nm) was deposited to a preliminarily cleaned (ultrasonication followed by ultraviolet irradiation) glass substrate by spray pyrolysis method. Metal electrodes of interdigital structure were deposited by resistive evaporation of aluminum through the mask.

The algorithm of the experiment consisted of two steps. First, samples were dehydrated at 120 °C for 1 h, and then placed in a chamber with a humid (RH 99%) environment. Humidity was measured using IVA-6A instrument. Monitoring of generated voltage dependence from time  $V=f(t)$  was carried out by Keithley 238 High-Current Source-Measure Unit in the microvoltmeter mode under the ohmic load  $R=1\text{ MOhm}$  with an interval of 1 min.

X-ray diffraction analysis of the samples was performed using an Empyrean diffractometer (PANalytical) with a high-temperature console. Spatial and structural organization of the samples was studied by the transmission (TEM) and scanning (SEM) electron microscopies on the JEM 200A and JSM640LV instruments, respectively.

## Results and discussion

### Structure of the device

A typical functional converter device is shown in Fig. 2. Its size is  $35\times 20\text{ mm}$  (area is  $700\text{ mm}^2$ ) and distance between electrodes is 0.75 mm.

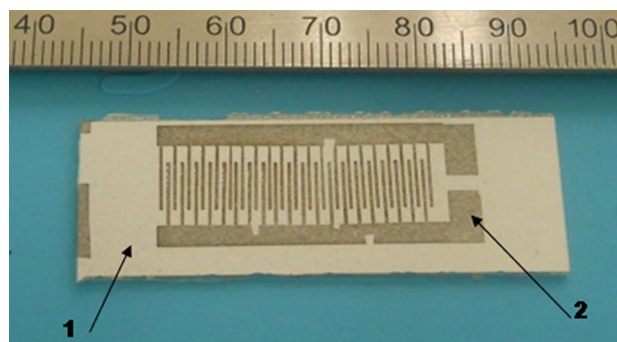


**Fig. 2** Planar structure of the chemo-electronic converter device, where 1 is the functional layer deposited on the glass substrate, and 2 is the interdigital contact structure

Cross-sectional SEM image of the obtained film is shown in Fig. 3 where the large number of pores of various sizes can be distinguished. Such pores promote an easy access of water molecules inside samples and hence allow interaction with  $\text{ZrO}_2$ -based nanomaterial. The porosity of the film ( $O$ ) is an important parameter of this device. The resistance to the flow of incoming gases limits the speed of chemo-electronic conversion, and consequently the output current  $I(t)=f(O)$  and the output power of the converter device  $W$ :

$$W = (R - r) (\int I(t) dt)^2 / T, \quad (1)$$

where  $T$ —the period of cycle;  $r$ —ohmic resistance of the polymer (internal resistance of the system);  $R$ —resistance of external load.

### The effect of chemo-electronic conversion

The time dependence of EMF generated after placing the sample in a humid atmosphere is shown in Fig. 4. It can be

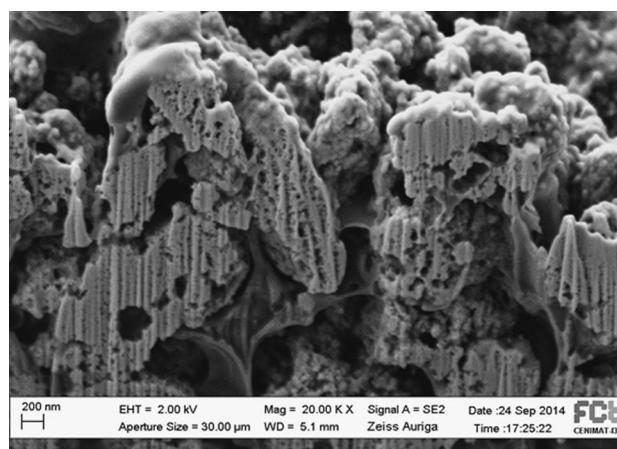


**Fig. 3** SEM cross-sectional image of deposited  $\text{ZrO}_2$ -3 mol%  $\text{Y}_2\text{O}_3$ /PVA film

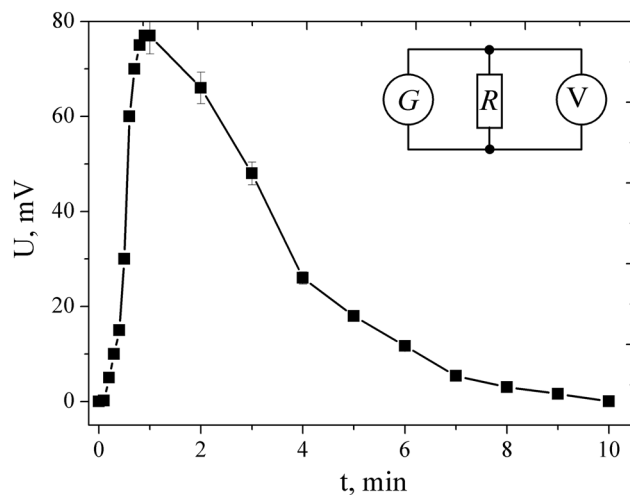


**Fig. 4** Variation of potential difference on the electrodes after device humidification with time at relative humidity of RH=99%, where *G* chemovoltaic cell, *R* electric load, *V* voltmeter

seen that the adsorption leads to an increase of the potential difference to about 80 mV after 2 min of the device humidification and its subsequent decrease to zero over the next 8 min.

The investigated chemovoltaic cell was tested under the load of 1 MΩ resistor. Consequently, it can be concluded unambiguously the flow an electric current  $I = U/R$  and performed work  $A = (U^2/R) t$  between the electrodes of converter device. It is easy to estimate the average-specific electrical power output of the device  $\langle P \rangle = \langle U \rangle^2 / RS$ .

$$\begin{aligned} \langle P \rangle &= (40 \times 10^{-3})^2 V^2 / 10^6 \text{ Ohm} \times 7 \times 10^{-4} \text{ m}^2 \\ &= 2.3 \times 10^{-6} \text{ W/m}^2. \end{aligned} \quad (2)$$

Such result coincides approximately with the power of known functional analogs based on electrostatic charge capture from microscopic water droplets (Miljkovic et al. 2014) ( $1.5 \times 10^{-11} \text{ W/cm}^2 = 1.5 \times 10^{-7} \text{ W/m}^2$ ) and on adsorption-induced electrostriction ( $5.6 \times 10^{-7} \text{ W}$ ) (Ma et al. 2013). The relatively high efficiency of nanopowder chemo-electronic converters is caused by direct conversion of chemical interaction energy into an electrical form, passing intermediate stages.

Also, it can be assumed that the occurrence of a flow of charge carriers in the space between the electrodes is caused by inhomogeneities in the height and density of the functional layer.

The X-ray spectra represented in Fig. 5 show the results of the measurements of the ZrO<sub>2</sub>-based nanopowder after saturation with moisture at room temperature for 12 h (curve 1), followed by stepwise heating to 400 and 500 K (curves 2 and 3) and after cooling in vacuum (curve 4).

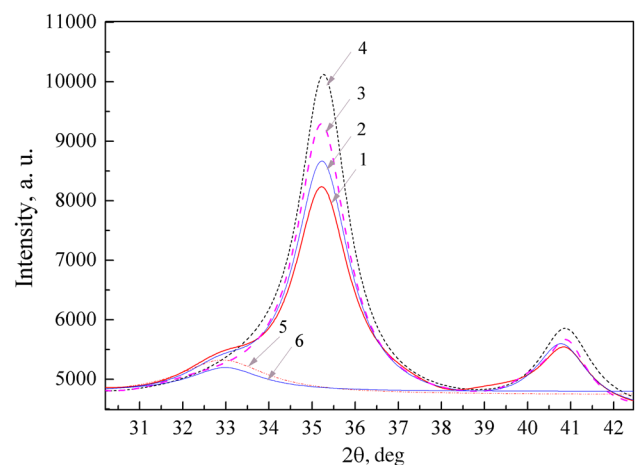


**Fig. 5** XRD spectra of the ZrO<sub>2</sub>-3 mol% Y<sub>2</sub>O<sub>3</sub> nanopowder, where 1—after saturation under humid environment at 300K for 24 h; 2—after drying at of 400 K for 30 min; 3—after drying at a temperature of 500 K for 30 min; 4—after cooling from 500 to 320 K under vacuum for 24 h; 5 and 6 are the peaks of the monoclinic phase, extracted from spectra 1 and 2

In contrast to the high peak of the tetragonal (T) phase (101), spectra 1 and 2 exhibit a weak peak of the monoclinic (M) phase (111) (Fig. 5, curves 5 and 6). For clarity, these peaks were selected programmatically from the spectra (curves 1 and 2). It is noteworthy that after cooling in a vacuum, the appearance of monoclinic phase peaks is not observed. Consequently, the T–M phase transition is not of a thermal but of adsorption nature.

According to the X-ray diffraction data, the adsorption of water molecules leads to destabilization of the high-temperature T-phase retained by the defective complexes of the impurity–vacancy dipole (IVD), type: Me–V<sub>O</sub>. These complexes are formed by ionized Y<sup>3+(-)</sup> impurity atoms and oxygen vacancies V<sup>(+)</sup> formed for the compensation of the charge caused by these impurity atoms (Naumov et al. 1992; Wert and Thomson 1969). Earlier, it was shown that the T–M phase transition is atypical for this class of materials and is realized in a limited volume, namely in the 2D layer near the surface (Konstantinova et al. 1996). In the work of Alekseenko and Volkova (1999), the questions of adsorption martensitic T–M transformation in Zr-ceramics were studied in details. Consequently, it can be assumed that the chemo-electron emission and T–M transformation processes discussed above are various forms of a single physical–chemical process that occurs on the surface of nanoparticles and in its near-surface layers. Moreover, this process is directly related to the electronic subsystem of nanoparticles. This statement is confirmed by the studies carried out on bulk nanostructured samples presented elsewhere (Doroshkevich et al. 2017a, b; Subhoni et al.

2018), where the proposed mechanism of the effect was described, the essence of which is as follows.

### Conversion mechanism

Upon contact of an electrically neutral surface (Fig. 6a) with a neutral water molecule, dissociative adsorption takes place. The water molecule dissociates under the action of the force field gradient of the active centers of the particle surface. Negatively charged hydroxyl (OH<sup>-</sup>) groups are chemically bounded on the surface and the saturation of free valence bonds occurs. As a result, the surface acquires a negative charge relative to the volume of the nanoparticle. This leads to the bending of the energy bands in the near-surface region of the nanoparticle material L (Fig. 6b). And where the upper levels of the valence band (the acceptor levels of the Y<sup>3+(-)</sup> impurity) intersect the Fermi level E<sub>F</sub> in a narrow area near the surface L' (Fig. 6, b), the electron is localized from the crystal lattice by the tunnel effect with a probability determined by the Fermi–Dirac function. The difference between the work function of ZrO<sub>2</sub> 3 mol%Y<sub>2</sub>O<sub>3</sub> A<sub>ZrO2</sub> = 3–5 eV, (Zainullina and Zhukov 2000) and the ionization energy of the water molecule A<sub>OH</sub> = 13.2 eV (Gurvich et al. 1974) is of ΔA = 8–10 eV; therefore, the electron density shifts outside the crystal aside to the adsorption layer.

The process of dissociative adsorption is a multi-stage process which includes the interaction of a certain number of water molecules through the formation and destruction of the complexes. During dissociation, some parts of the

ions practically exist in a free state and in the presence of a gradient of the electric field ensure the transportation of the charges to the electrodes.

The end of the electron emission process occurs when the uncompensated valence bonds are saturated. Thus, the system has a specific physical limit on the production of charge carriers. The electrical and adsorption capacity of the system is determined by the permittivity of the material ε and the chemical activity of the surface and in case of ZrO<sub>2</sub>-based nanoparticles obtained by the chemical method is relatively high (ε = 25).

A schematic explanation of the adsorption mechanism of the T–M transformation is shown in Fig. 7.

As can be seen from Fig. 7, the charge exchange of crystal lattice ions due to adsorption-induced electron emission leads to the change in the interaction length of the impurity ion and the oxygen vacancy. Since the adsorption weakens the effect of the alloying element, in the local volume of the material near the surface, the structure becomes monoclinic, which is natural for ZrO<sub>2</sub> at room temperature.

### Conclusion

The results of structural studies confirm the proposed mechanism of chemo-electronic conversion, which assumes electron emission from the material of nanoparticles. It can also be concluded that IVD plays a key role in the generation of electrical charges. They provide a high density of shallow levels E<sub>a</sub> ≤ 0.2–0.4 eV, near the Fermi level E<sub>F</sub> and become

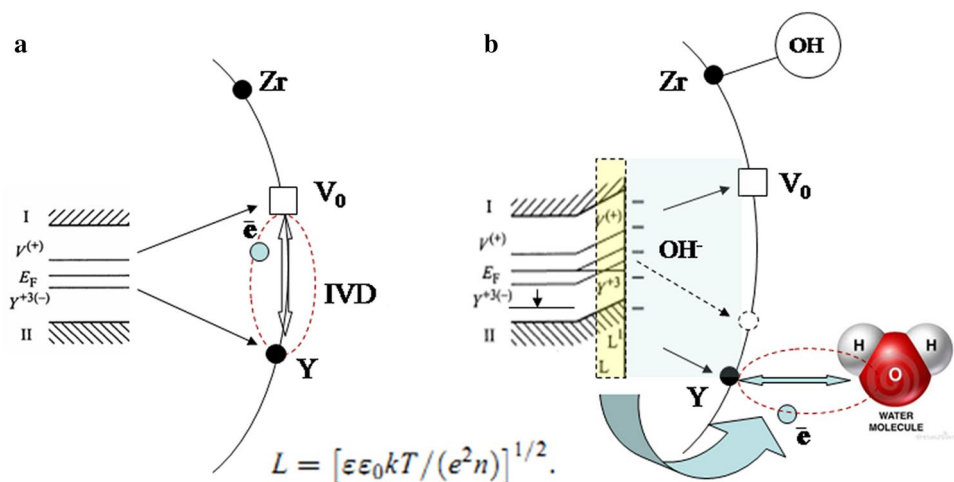
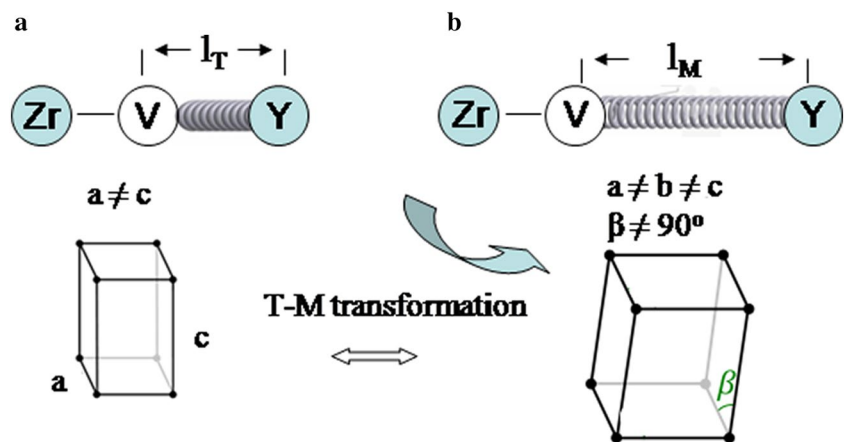


**Fig. 6** Schematic representation of the adsorption mechanism of electron emission. System before (a) and after (b) adsorption of water molecules, where: I—conduction band, II—valence band, OH<sup>-</sup>—negatively charged hydroxyl groups, Y<sup>+3(-)</sup>—the acceptor level corresponding to the surface Y atom, V<sup>+</sup>—is the donor level corresponding to the oxygen vacancy V<sub>o</sub>, L—the length of the region where

the local curvature of the energy levels exists, L'—the length of the region where the yttrium acceptor level Y<sup>+3(-)</sup> crosses the Fermi level E<sub>F</sub>. L is determined by the dielectric constant of the material ε and the concentration of charge carriers n (20). k—the Boltzmann constant, e—the electron charge

**Fig. 7** Schematic representation of the adsorption mechanism of the T–M transformation. The system before (a) and after (b) the adsorption of water molecules, where  $l_T$  and  $l_M$  are the chemical bond length of the IVD in T and M—structural modifications, respectively



a potential source of electrons. It should be noted that one more circumstance was discovered recently (Oksengendler et al. 2010a, b, 2017). It turned out that on the curved nanoscale surfaces with a pronounced ionic bond, the energy of Tamm states depends on the curvature of the surface. This new phenomenon, called nanofractality (Oksengendler et al. 2017, 2018), in principle allows to control the location of the density of the surface states in the bandgap, i.e. optimize the effects discussed in this article.

**Acknowledgements** The authors thank Dr. R.G. Nazmitdinov (JINR), Dr Y.B. Martynov and Dr. P.P. Gladyshev from Dubna State University, Dr N.A. Poklonsky (BSU) for discussion results. Results presented here received funding from the European Union Horizon 2020 research and innovation program under the Marie Skłodowska Curie Actions Grant agreement 691010, also JINR-Romania Cooperation Programme Project of 2018 Order no. 323/65, Project No. 323/21.05.2018 item 68 and RFBR Grant no. 17-52-45062.

**Author contributions** DAS—analysis of the results, preparation of the manuscript, development of the empirical mechanism of the chemo-electronic conversion effect. AEB—XRD experiment, mathematical processing of results, discussion of experimental results. ShAV—engineering of chemo-electronic device, preparing a manuscript, discussing the results of the experiment. LAI—SEM research of the samples, discussion of the experimental results. LAI—conducting electrical studies of samples, discussion of experimental results. GVA—TEM research samples, discussion of the experimental results. IAKh—comprehensive analysis of the results, analysis of the mechanism of the chemo-electronic conversion effect from the standpoint of the theory of polymolecular adsorption. TVA—XRD research of samples in vacuum, discussion of the results of the experiment. AV—comprehensive analysis of the results, discussion of the mechanisms of charge delivery to the electrodes. LD—comprehensive analysis of the results, discussion of the mechanisms of electron emission and charge delivery to electrodes. BM—development of an empirical mechanism for the effect of chemo-electronic conversion. DVS—production of nanopowders, development of methods for obtaining working suspensions for chemo-converters, discussion of the mechanism of the effect of chemo-electronic conversion from the standpoint of the theory of interfacial catalysis. MAI—conduct a literature review, discuss the results of the experiment experiment from the standpoint of physical chemistry. KKT—discussion of the mechanism of delivery of charge carriers to the electrodes from the standpoint of molecular dynamics. BVI—discussion of the mechanism

of the chemo-electronic conversion effect as from the standpoint of the theory of catalysis on the surface of semiconductors, discussion of the results of the experiment. OBL—discussion of the empirical mechanism of the effect of chemo-electron conversion from the standpoint of band theory and the theory of nanofractality, discussion of the results of the experiment.

## Compliance with ethical standards

**Conflict of interest** The authors declare that they have no competing interests.

## References

- Alekseenko VI, Volkova GK (1999) Adsorption mechanism of phase transformation in stabilized zirconia. *J Tech Phys* 70:57–62
- Doroshkevich AS, Danilenko IA, Konstantinova TE (2006) Diagnostics of nanopowder systems based on zirconia by transmission electron microscopy. *Electron Microsc Strength Mat* 13:151–159
- Doroshkevich AS, Lyubchik AI, Islamov AK (2017a) Nonequilibrium chemo-electronic conversion of water on the nanosized YSZ: experiment and molecular dynamics modelling problem formulation. *J Phys Conf Ser* 848(012021):1–9. <https://doi.org/10.1088/1742-6596/848/1/012021>
- Doroshkevich AS, Lyubchik AI, Shilo AV (2017b) The effect of chemo-electronic energy conversion in nanopowder systems based on zirconia. *Surf X-Ray Synchrotron Neutron Stud* 11(3):523–529. <https://doi.org/10.1134/S1027451017030053>
- Gergen B, Nienhaus H, Henry Weinberg W, Mc Farlandand EW (2001) Chemically induced electronic excitations at metal surfaces. *Science* 294:2521–2523. <https://doi.org/10.1126/science.1066134>
- Gurvich LV, Karachevtsev GV, Kondratiev VN et al (1974) Breaking energies of chemical bonds, ionization potentials and electron affinity. *Sci Moscow* 351:276
- Kabansky AY, Styrov VV (2004) A new means of chemical energy conversion by semiconductor. In: Chandra D, Bautista RG, Shlapbach L (eds) *Adv Mat for energy conversion II*. TMS, Charlotte, pp 43–52
- Kabansky AY, Styrov VV, Tyurin YI (1979) On the possibility of direct conversion of chemical energy into electrical energy on semiconductors. *Lett ZhTF* 5:833–836
- Kammler Th, Kupperts J (1999) Interaction of H atoms with Cu(111) surfaces: adsorption, absorption, and abstraction. *J Chem Phys* 111:8117. <https://doi.org/10.1063/1.480145>

- Konstantinova TE, Volkova GK, Danilenko IA (1996) Features of the tetragonally monoclinic transformation in the surface layers of the ceramics of the  $ZrO_2$ - $Y_2O_3$  system. *PHPT* 6:9–19
- Konstantinova T, Danilenko I, Glazunova V, Volkova G, Gorban O (2011) Mesoscopic phenomena in oxide nanoparticles systems: processes of growth. *J Nanopart Res* 13:4015–4023. <https://doi.org/10.1007/s11051-011-0329-8>
- Ma M, Guo L, Anderson DG, Langer R (2013) Bio-inspired polymer composite actuator and generator driven by water gradients. *Science* 339:186–189. <https://doi.org/10.1126/science.1230262>
- Miljkovic N, Preston DJ, Enright R, Wang EN (2014) Jumping-droplet electrostatic energy harvesting. *Appl Phys Lett* 105:013111. <https://doi.org/10.1063/1.4886798>
- Muller J, Rech B, Springer J (2004) TCO and light trapping in silicon thin film solar cells. *Sol Energy* 70:917. <https://doi.org/10.1016/j.solener.2004.03.015>
- Naumov II, Olkhovsky GA, Velikokhatny OI, Aparov NN (1993) The mechanism of stabilization of the cubic phase  $ZrO_2$ . *Solid State Phys* 35:1089–1091
- Okamoto Y (2008) First-principles molecular dynamics simulation of  $O_2$  reduction on  $ZrO_2$  (111) surface. *Appl Surf Sci* 255:3434–3441. <https://doi.org/10.1016/j.apsusc.2008.09.061>
- Oksengendler BL, Turaeva NN (2010a) Surface tamm states at curved surfaces of ionic crystals. *Dokl Phys* 434:609
- Oksengendler BL, Turaeva NN (2010b) Surface tamm states at curved surfaces of ionic crystals. *Dokl Phys* 55:477–479
- Oksengendler BL, Askarov B, Nikiforov VN (2014) Role of electron confinement in the formation of Tamm surface levels in nanoparticles. *ZhTF* 84:156
- Oksengendler BL, Nikiforov VN, Maksimov SE (2017) Tamm states of fractal surfaces. *Rep Acad Sci* 744(4):423–426. <https://doi.org/10.7868/S0869565217040053>
- Oksengendler BL, Maksimov SE, Nikiforov VN (2018) Surf X-Ray Synchrotron Neutron 2:68–73 <https://doi.org/10.7868/S0207352818020117>
- Ptitsyn VE (2007) Anomalous thermal field emission. *ZhTF* 77(4):113–118
- Styrov VV, Simchenko SV (2012) High-efficiency generation of electron–hole pairs on a selenium p–n junction under the action of atomic hydrogen. *ZhTF Lett* 96:343–346
- Styrov VV, Simchenko SV (2013) Generation of chemo-EMF in a nanoscale pn-junction based on SiC. *Rep Natl Acad Sci Ukraine* 5:80–86
- Styrov VV, Tyurin YI (2003) Nonequilibrium chemoeffects on the surface of solids. *Energoatomizdat, Moscow*
- Styrov VV, Simchenko SV, Golotyuk VN (2011) Chemo-EMF in the silicon solar cell exposed to low-energy hydrogen atoms. *Nanomat Appl Prop* 2(1):85–91
- Subhoni M, Kholmurodov K, Doroshkevich A, Asgerov E et al (2018) Density functional theory calculations of the water interactions with  $ZrO_2$  nanoparticles  $Y_2O_3$  doped. *J Phys Conf Ser* 994:012013. <https://doi.org/10.1088/1742-6596/994/1/012013>
- Tyurin YI, Horuzhy VD, Shigalugov, SK et al (2008) Efficiency of transmission of energy of adsorption and recombination of atoms to the solid body at different mechanisms of excitation. *News Tomsk Pol Univ* 312:56–65
- Wert C, Thomson R (1969) *Solid state physics*. Mir, Moscow, p 280
- Zainullina VN, Zhukov VP et al (2000) Electronic structure and ion characteristics conductivity in zirconium dioxide, stabilized calcium and yttrium impurities. *Zh Strukt Khim* 41(2):229–239
- Zheng L, Ma Y, Chu S (2014) Improved light absorption and charge transport for perovskite solar cells with rough interfaces by sequential deposition. *Nanoscale* 6:8171. <https://doi.org/10.1039/c4nr01141d>

**Publisher's Note** Springer Nature remains neutral with regard to jurisdictional claims in published maps and institutional affiliations.